

Spectral response analysis of PVDF capacitive sensors

B. Reyes-Ramírez^{*}, C. García-Segundo, A. García-Valenzuela

Centro de Ciencias Aplicadas y Desarrollo Tecnológico, Universidad Nacional Autónoma de México, Ciudad Universitaria, Coyoacán, Apartado Postal 70-186, Distrito Federal 04510, México.

Correspondent author: bartolome.reyes@ccadet.unam.mx

Abstract. We investigate the spectral response to ultrasound waves in water of low-noise capacitive sensors based on PVDF polymer piezoelectric films. First, we analyze theoretically the mechanical-to-electrical transduction as a function of the frequency of ultrasonic signals and derive an analytic expression of the sensor's transfer function. Then we present experimental results of the frequency response of a home-made PDVF in water to test signals from 1 to 20 MHz induced by a commercial hydrophone powered by a signal generator and compare with our theoretical model.

1. Introduction.

It is known that the optical absorption of pulsed or modulated light, prompts elastomechanical perturbations via non-radiative processes. This is the so-called photoacoustic effect [1]. For each pulse of light, the energy conversion associated to the non-radiative processes remains confined to the interaction volume, inducing a short-living local increase of pressure (thermo-elastic expansion). Then this propagates through the bulk as an elastomechanical perturbation. I.e. a photoacoustic perturbation propagates through the sample as sound. The frequency dominion of the so-induced perturbations is in the ultrasonic range and can cover from say 100 KHz and up to several hundreds of MHz depending upon the physical properties of the sample. By sample we mean the media where the optical to elastomechanical energy conversion takes place. The registering of this photoacoustic perturbations demands the use of tailored ultrasonic sensors. Due to the high sensitivity and the heavy performance conditions as required, the most frequent sensors used for this purpose are ultrasonic transducers based on PZT-piezoelectric ceramics [2]. These are quite reliable, stable and broadly used in scientific and technical sensing applications [1, 2]. However, they present some limitations in terms of performance and their manufacture process for photoacoustic applications such as: full registering of information at short time constant [3], or for arrays of ultrasonic sensors with specific morphologies and wide bandwidth spectral response as these required in photo-acoustic imagenology [4, 5]. An alternative for manufacturing the required ultrasound sensors and assembling arrays of them is the use of pyroelectric and piezoelectric Polyvinylidene fluoride (PVDF) films in capacitive configuration. The PVDF's piezoelectric component offers a much broader bandwidth window than PZT ceramics [2, 5-7]. With PVDF films at hand, targeted designs of sensing structures are at reach for covering specific sensing needs in pulsed photo-acoustic imaging [4, 5,7]. Indeed one of the first concerns that arise when designing sensors for such a broad bandwidth is their spectral response quality. In general it is very difficult, if not impossible, to have a flat non-negligible response over a spectral range of many MHz. Because as the frequency of sound increases the wavelength decreases, above certain frequency the



wavelength inside the PVDF slab is smaller than the thickness and resonances are to be expected. For ultrasound frequencies up to 50 MHz, the wavelength of sound will be smaller than many piezoelectric film sensors. We have not found in the literature explicitly an expression for the frequency dependent transfer function of film piezoelectric capacitive sensors. In this paper we derive an expression for transfer functions assuming ultrasound is incident normally on a piezoelectric film. Then we compare measurements performed on a home-made PVDF capacitive sensor in the frequency range from 1 to 20 MHz.

2. Theoretical analysis

The piezoelectric materials are anisotropic dielectric materials. In these materials an electric field \mathbf{E} induces a dipolar moment on the constituent molecules, which is proportional to this electric field. The contribution to the total electrical dipolar moment per unit volume (\mathbf{P}), resulting from the applied electric field and in the absence of mechanical stress, can be written as, $\mathbf{P}_E = \epsilon_0 \vec{\chi}_e \cdot \mathbf{E}$. Where $\vec{\chi}_e$ is the electrical susceptibility tensor and ϵ_0 is the electrical permittivity of the vacuum. The mechanical stress field, \mathbf{S} , also contributes to the induced dipolar moment per unit volume in piezoelectric materials. Within the linear response regime of the material and in the absence of an electric field, the contribution to \mathbf{P} by mechanical stress is written as, $\mathbf{P}_S = \vec{d} \cdot \mathbf{S}$. Here \vec{d} is the piezoelectric tensor. However, in the presence of small electric and stress fields, the electrical polarization per unit volume in the piezoelectric is simply the sum of \mathbf{P}_E and \mathbf{P}_S . As result, in a piezoelectric material we have that,

$$\mathbf{P} = \vec{d} \cdot \mathbf{S} + \epsilon_0 \vec{\chi}_e \cdot \mathbf{E}. \quad (1)$$

We assume that the stress field and electric field have amplitudes small enough so that neither field affects the piezoelectric tensor or the susceptibility tensor; see figure 1 for schematic visual guidance. Notice that when the pressure perturbation impinges on the slab on the normal direction respect the piezoelectric surface, the stress field inside the slab has all components equal to zero except the S_{33} component, which turns out to be,

$$S_{33} = \psi_{\text{int}}(z, t). \quad (2)$$

Thus, the stress field acting on the electrical polarization vector of the piezoelectric materials produces component along the z axis; given by $P_{23} = d_{33} S_{33}$ while the electrical polarization induces a charge density and a surface charge density according to the following relations, $\nabla \cdot \mathbf{P}(r, t) = -\rho_b(r, t)$ and $\mathbf{P}(r, t) \cdot \hat{n} = \rho_s(r, t)$. Here \hat{n} is the unit outward normal to the piezoelectric surfaces. Then the stress-induced charge densities are,

$$\rho_b(r, t) = -\nabla \cdot (d_{33} S_{33} \hat{a}_z) = -d_{33} \frac{\partial S_{33}}{\partial z}, \quad \rho_z^{(0)} = -d_{33} S_{33} \Big|_{z=0} \text{ and } \rho_z^{(d)} = -d_{33} S_{33} \Big|_{z=d}.$$

As a result one obtains that the field within the slab is,

$$E_z^s(z) = \left[-\frac{d_{33}}{\epsilon} S_{33}(z) - \frac{d_{33}}{\epsilon} \left[\frac{S_{33}(h) + S_{33}(0)}{2} \right] \right]. \quad (3)$$

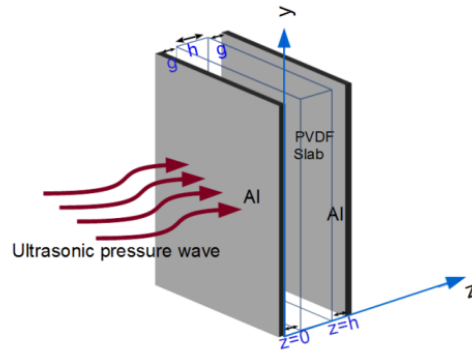


Figure 1. Schematic diagram of transduction from ultrasonic pressure perturbation to electric signal.

For the condition in which the piezoelectric slab is between two flat metallic electrodes, e.g. forming a parallel-plate capacitor (see figure 1), the electrodes are charged with a surface density $\rho_s^{(e)}$ and an electric field is produced between the electrodes. This electric field induces also the polarization of the piezoelectric slab. The electric field and polarization induced by the charges on the electrodes simply adds up with the electric field and with polarization induced by the stress. Within the gaps of width g , shown in the figure above, the electric field due to the electrode charges is normal to the interfaces with amplitude, $E_z^{(e)} = \rho_s^{(e)} / \epsilon_0$. Within the piezoelectric slab the electric field is also in the z direction and of amplitude $E_z^{(e)} = \rho_s^{(e)} / \epsilon$. The total electric field inside the piezoelectric slab is,

$$E_z(z) = -\frac{d_{33}}{\epsilon} S_{33}(z) - \frac{d_{33}}{\epsilon} \left[\frac{s_{33}(h) + s_{33}(0)}{2} \right] + \rho_s^{(e)} / \epsilon. \quad (4)$$

By letting the gaps tend to zero, the electric potential difference between the electrodes is then obtained as,

$$E_z(z) = \frac{Q_e h}{A \epsilon} + \frac{d_{33} h}{\epsilon} \left[\frac{s_{33}(h) + s_{33}(0)}{2} \right] + \int_0^h \frac{d_{33}}{\epsilon} [S_{33}(z)] dz. \quad (5)$$

On the other hand, when a monochromatic plane ultrasonic wave is incident normally to the sensor, the ultrasonic pressure perturbation inside the piezoelectric slab is $\psi_a + \psi_b$, where $\psi_a = A(\omega) \psi_i e^{j(\omega t - k_2 z)}$, $\psi_b = B(\omega) \psi_i e^{j(\omega t + k_2 z)}$, ψ_i the amplitude of the incident pressure $k_2 = 2\pi/\lambda_2 = \omega/c_2$. In the latter expression λ_2 is the wavelength, c_2 is the phase velocity of sound in the piezoelectric and $\omega = 2\pi f$, with f being the frequency of the incident ultrasonic wave. Thus the amplitudes in the perturbation within the slab are given by,

$$A(\omega) = \frac{[1 + r_{21}]}{1 - r_{21} r_{23} e^{-2jk_2 h}} \quad \text{and} \quad B(\omega) = \frac{-r_{23} [1 + r_{21}] e^{-2jk_2 h}}{1 - r_{21} r_{23} e^{-2jk_2 h}}, \quad (6)$$

where, $r_{21} = (z_2 - z_1)/(z_2 + z_1)$ and $r_{32} = (z_2 - z_3)/(z_2 + z_3)$, are the reflection coefficients at normal incidence at the interfaces between the slab (medium 2) and the incidence medium (medium 1, for $z < 0$) and the interface between the slab and the transmission medium (medium 3, $z > h$), respectively; where z_1 , z_2 and z_3 are the acoustic impedance of medium 1, 2 and 3, respectively. We then have,

$$V_c = \frac{Q_e}{C_0} + \frac{d_{33}h}{\varepsilon} \left[\frac{A(\omega)[e^{-jk_2h} + 1] + B(\omega)[e^{jk_2h} + 1]}{2} \right] \psi_i + \int_0^h \frac{d_{33}}{\varepsilon} [\psi_a(z) + \psi_b(z)] dz, \quad (7)$$

where $C_0 = \varepsilon A / h$ is the electrical capacitance. Performing the integrals yields,

$$V_c = \frac{Q_e}{C_0} + \frac{d_{33}h}{\varepsilon} \left[\frac{A(\omega)[e^{-jk_2h} + 1] + B(\omega)[e^{jk_2h} + 1]}{2} \right] \psi_i + \frac{d_{33}}{\varepsilon} \left[\frac{A(\omega)[e^{-jk_2h} - 1]}{-jk_2} + \frac{B(\omega)[e^{jk_2h} - 1]}{jk_2} \right] \psi_i.$$

Notice that the factor $\exp(j\omega t)$ is implicit in all terms. Clearly the equivalent circuit is a capacitor C_0 in series with a voltage source V_s given by,

$$V_s(\omega) = \frac{d_{33}h}{2\varepsilon} \left\{ A(\omega) \left[e^{\frac{-j\omega h}{C_2}} + 1 \right] + B(\omega) \left[e^{\frac{j\omega h}{C_2}} + 1 \right] \right\} \psi_i + j \frac{d_{33}C_2}{\omega\varepsilon} \left\{ A(\omega) \left[e^{\frac{-j\omega h}{C_2}} - 1 \right] - B(\omega) \left[e^{\frac{j\omega h}{C_2}} - 1 \right] \right\} \psi_i$$

where we used $k_2 = \omega / c_2$. If we connect the circuit to an oscilloscope we add an impedance in series and close the circuit. The voltage drop across the input impedance of the oscilloscope is, $V_{osc} = IZ_i$, while the voltage drop across the piezoelectric capacitor must be zero. Thus we get,

$$V_{osc} = \frac{-Z_i}{-Z_i + \frac{1}{j\omega C_0}} V_s. \quad (8)$$

If we define the transfer function as,

$$H(\omega) = \frac{V_{osc}(\omega)}{\psi_i(\omega)}, \quad (9)$$

we get,

$$H(\omega) = \frac{-Z_i(\omega)}{-Z_i(\omega) + \frac{1}{j\omega C_0}} \left\{ \frac{d_{33}h}{2\varepsilon} \left[A(\omega) \left(e^{\frac{-j\omega h}{C_2}} + 1 \right) + B(\omega) \left(e^{\frac{j\omega h}{C_2}} + 1 \right) \right] + j \frac{d_{33}C_2}{\omega\varepsilon} \left[A(\omega) \left(e^{\frac{-j\omega h}{C_2}} - 1 \right) - B(\omega) \left(e^{\frac{j\omega h}{C_2}} - 1 \right) \right] \right\} \quad (10)$$

This is our result for the transfer function of a film piezoelectric capacitor transducer for normally incident ultrasound. For incidence at angles different from normal, the Eq. (2) would be expressed in terms of the corresponding angular projection and its implications shall be cascaded over the calculation up to reaching an expression equivalent to Eq. (10).

3. Numerical Example

In Fig. 2 we plot the magnitude of the transfer function given in Eq. (10) versus the angular frequency ω from 1 MHz to 20 MHz for a 100 μm thick PVDF film immersed in air, water and in a medium of

the same acoustic impedance as that of the PVDF (a perfect impedance match). To generate the curves in Fig. 2 we assumed the speed of sound in air, water and in the PVDF is 343 m/s, 1484 m/s, and 2200 m/s respectively, and we supposed the corresponding densities are 1000 g/cm³, 1593 g/cm³ and 1780 g/cm³, respectively.

We can appreciate that the transfer function predicted by Eq. (10) sinks at about 13 MHz. This is a result of destructive interference of the multiply reflected ultrasound waves within the PVDF film. Note that the difference between the spectral response of the sensor in water and with a perfect impedance match is negligible.

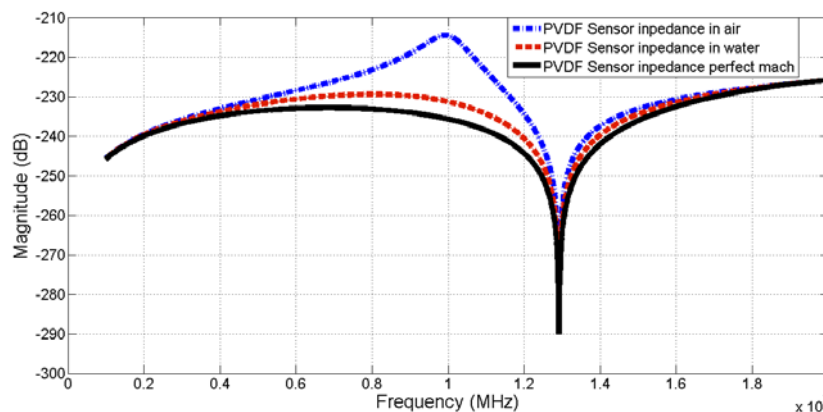


Figure 2. Plot of analytic calculations for $|H(\omega)|$ as a comparison from different media (air, water, PVDF).

4. Comparison with experimental measurements.

We fabricated a PVDF capacitor sensor by depositing very thin layers of aluminum on the surfaces of a 110 μm thick PVDF film and connecting it to a voltage preamplifier (ONDA, model HA-1100). The sensors were sealed with a thick plastic coating for its protection. The sensitive area of the PVDF capacitor was 3 mm². The capacitor sensor was immersed in a bucket filled with water and the signal generated by a calibrated commercial hydrophone emitting ultrasound waves towards the sensor was registered with an oscilloscope.

In Fig. 3 we show the sensor's frequency response and the prediction of Eq. (10) above. The experimental response is somewhat different to the theoretical curve, but this is expected since Eq. (10) does not include the effects of the electrodes nor sealant coating that covers on the real sensor. Nevertheless we can see in the experimental curve a drop at 13 MHz as predicted by the model. This is only a preliminary result and of course, a broader analysis and more experiments are needed to improve the sensors response as demanded in photo-acoustic imaging applications. Nevertheless, the model derived here is a necessary tool for developing low-noise ultrasonic sensors with broad frequency response range, as required. We are currently working on a comprehensive experimental characterization of our PVDF sensors of different thicknesses and on the extension of our model.

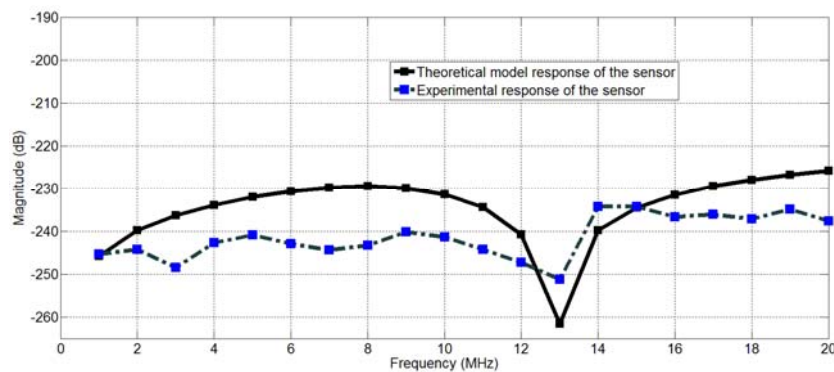


Figure 3. Comparison of the frequency response of the sensor and Eq. (10).

5. Conclusions

We derived an analytic expression for the transfer function of a piezoelectric capacitor sensor taking into account multiple reflections of ultrasonic waves within the sensor. It was found that dips in the transfer function arise due to interference effects. We obtained experimental data on the frequency response of a 110 mm thick PVDF sensor and observed a dip around 13 MHz as predicted by the theoretical model. The possible relevance of these dips on the sensors performance in photo-acoustic imaging is currently under assessment.

Acknowledgments

We acknowledge financial support from Dirección General de Asuntos del Personal Académico of Universidad Nacional Autónoma de México through grant PAPIIT IN-106712 and to Instituto de Ciencia y Tecnología from Ciudad de México for the partial support of this work through a breast cancer research contract.

References

- [1]. C. K. N. Patel and A. C. Tam: Pulsed optoacoustic spectroscopy of condensed matter, *Rev. Mod. Phys.* 53, 517 (1981).
- [2]. G. L. Messing, S. Trolier-McKinstry, E. M. Sabolsky, C. Duran, S. Kwon, B. Brahmaroutu, P. Park, H. Yilmaz, P. W. Rehrig, K. B. Eitel, E. Suvaci, M. Seabaugh, and K. S. Oh.: "Templated grain growth of textured piezoelectric ceramics". *Critical Reviews in Solid State and Materials Sciences* 29, 45–96 (2004).
- [3]. "Experimental observations of optically induced non-radiative fast-pulses in metals": C. García-Segundo, A. J. Smith, and J.-P. Connerade. *J. Modern Optics*. Vol. 51, 233 (2004).
- [4]. V. Moock, C. García-Segundo, E. Garduño and F. Arámbula-Cosío: "Signal Processing for Photoacoustic Tomography". *Proceedings of the 5th International Conference on Image and Signal Processing and 5th International Conference on BioMedical Engineering and Informatics (5th CISP'12 / IEEE-BMEI'12)*. Chongqing, China. 16-18 Oct. 2012, pp. 957 – 961. DOI: 10.1109/CISP.2012. 6469836.
- [5]. G. Paltauf, R. Nuster, S. Gratt: "Photoacoustic section imaging with integrating detectors". *ALT'12 Conference Proceedings*. Thun, Switzerland 2-6 September, 2012. DOI: 10.12684/alt.1.93.
- [6]. G. Gautschi: *Piezoelectric Sensorics: Force, Strain, Pressure, Acceleration and Acoustic Emission Sensors, Materials and Amplifiers*. Springer, 5-9 (2012).
- [7]. T. DH, Foster FS.: Fabrication and characterization of transducer elements in two-dimensional arrays for medical ultrasound imaging, *IEEE Trans Ultrason Ferroelectr Freq Control*, 39(4):464-75 (1992).